Liquid Crystals
Publication details, including instructions for authors and subscription information:
http://www.informaworld.com/smpp/title~content=t713926090

Second harmonic generation in ferroelectric liquid crystals and their mixtures

K. Yoshino[a]; M. Utsumi[a]; Y. Morita[a]; Y. Sadohara[a]; M. Ozaki[a]
[a] Department of Electronic Engineering, Faculty of Engineering, Osaka University, Suita, Osaka, Japan

To cite this Article Yoshino, K. , Utsumi, M. , Morita, Y. , Sadohara, Y. and Ozaki, M.(1993) 'Second harmonic generation in ferroelectric liquid crystals and their mixtures', Liquid Crystals, 14: 4, 1021 — 1032
To link to this Article: DOI: 10.1080/02678299308027809
URL: http://dx.doi.org/10.1080/02678299308027809

Liquid Crystals, 1993, Vol. 14, No. 4, 1021–1032

Second harmonic generation in ferroelectric liquid crystals and their mixtures

by K. YOSHINO*, M. UTSUMI, Y. MORITA, Y. SADOHARA
and M. OZAKI

Department of Electronic Engineering, Faculty of Engineering,
Osaka University, 2-1 Yamada-Oka, Suita, Osaka 565 Japan

The second harmonic generation (SHG) in the ferroelectric liquid crystal (FLC) state has been studied as functions of electric field strength, rotating angle, temperature and molecular structure. It has been confirmed that a sharp angularly phase-matching curve of the SHG controlled by an electric field is observed even in the liquid crystal. The temperature dependences of the phase-matched SHG and Maker fringe in the ferroelectric phase have also been studied, and temperature dependences of non-linear optical coefficients obtained. The SHG in several kinds of FLC and dye doped FLC have also been measured, and the enhancement of SHG realized by means of doping the FLC with several kinds of dye.

1. Introduction

Non-linear optical effects have attracted considerable attention from both fundamental and practical points of view. One of the simplest non-linear optic effects is second-harmonic generation (SHG). SHG is observed in crystalline material in which a centre of inversion symmetry is absent. Recently, a high efficiency of SHG has been confirmed for organic materials such as 2-methyl-4-nitroaniline (MNA) and *N*-(4-nitrophenyl)-L-prolinol (NPP) [1, 2]. In liquid crystals, mainly in nematic liquid crystals, only third harmonic generation has been studied [3], because in these compounds the centre of inversion symmetry still remains, except for some special cases such as a thin film in which the existence of the surface lowers the symmetry [4].

On the other hand, recently, ferroelectric liquid crystal (FLC) materials have been developed for high speed display devices [5]. In these compounds, to realize the ferroelectricity, a chiral carbon has been introduced into their molecular structures by which the centre of inversion symmetry has been lost. Therefore, a FLC is expected to be an active material for SHG. In addition, the tilt direction of the FLC molecules can be switched by the reversal of the polarity of an applied field and the response time of this switching is very short. Therefore, high speed modulation of SHG can be expected in the FLC device.

Some studies on SHG in FLCs have been carried out [6–8] and the angularly phase-matched SHG has also been reported [9–14]. However, the SHG signal was very weak and few systematic studies on SHG in FLC have been carried out [15]. Recently, attempts to design the optimum molecular structure for SHG have been made [16, 17]. In this paper, we report a detailed study on SHG in the FLC phase as functions of electric field strength, rotating angle, temperature, molecular structure and other parameters. The doping effect of some dye on FLCs is also studied.

---

* Author for correspondence.

2. Experimental

The molecular structures of the FLC used in this study are shown in figure 1. The preparation methods and the fundamental electric and optical properties of these compounds have previously been reported [18–23]. The compound mainly used for detailed studies such as temperature and angular dependences was (2S, 3S)-3-methyl-2-chloropentanoic acid $4',4''$-octyloxybiphenyl ester (3M2CPOOB) [18, 19].

The sample was sandwiched between two glass plates whose surfaces had been treated by a silane coupler (AY43-021, Toray Dow Corning Silicone) to obtain the homeotropic alignment for SHG measurement. Aluminium or stainless steel sheets of 10–260 μm thickness were used as electrodes and spacers. The separation between electrodes was typically 1 mm.

The cell configuration for SHG measurement is shown in figure 2. For measurement of the angularly phase-matched SHG, the sample cell was rotated around the

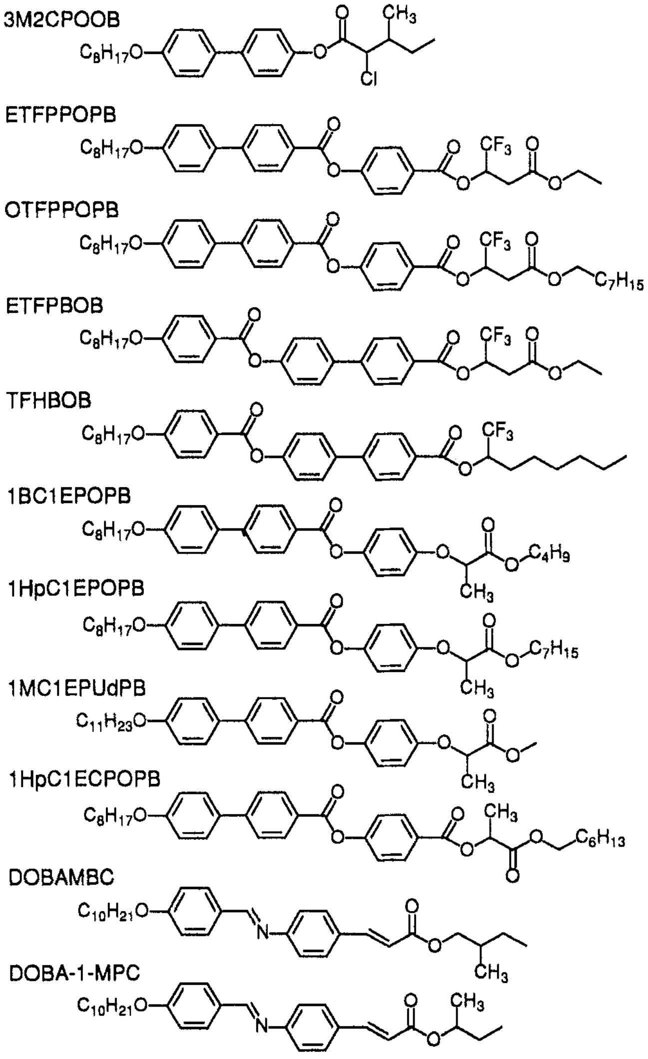

Figure 1. Molecular structures of ferroelectric liquid crystal materials used in this study.

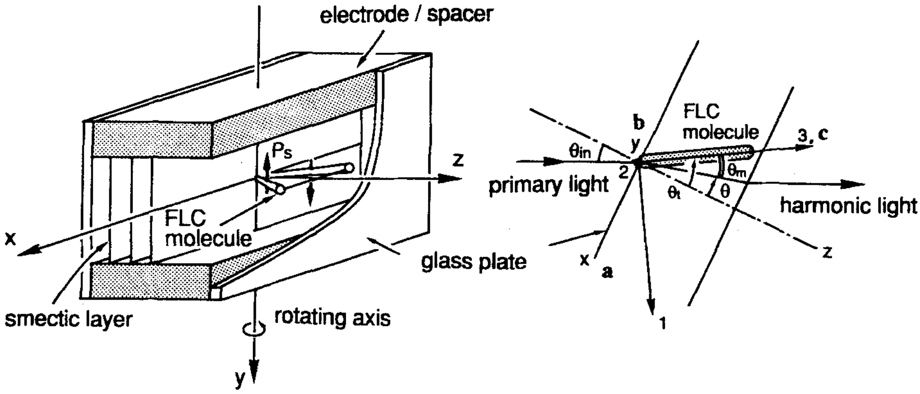

(a) (b)

Figure 2. Cell configuration for the measurement of the SHG.

y axis parallel to an electric field E. The fundamental light impinged on the cell perpendicular to the rotating axis (y) and propagated in the xz plane. The rotating angle θ was defined as the angle between the glass plate normal (z) and the propagation direction of the fundamental light in the liquid crystal. The angle θ was corrected using the equation, $\theta = \sin^{-1}(\theta_{\text{in}}/n_g)$, where θ_{in} is the angle between the glass plate normal and the direction of the incident light in air, and n_g is the refractive index of the glass ($n_g = 1{\cdot}51$ for 1064 nm). The refraction at the glass–liquid crystal interface was neglected.

A Q-switched Nd–YAG pulsed laser (wavelength: 1·064 μm, pulse width: 10 ns) was used as the fundamental light source after passing through a visible cut filter, polarizer and $\lambda/2$ plate. The fundamental beam was weakly focused by a lens ($f = 300$ mm). The generated harmonic light (532 nm) was monitored from the rear of the sample cell with a photomultiplier after passing through the analyser. To eliminate the fundamental light, infrared cut filters and an interference filter at wavelength 532 nm were installed in front of the photomultiplier. The detected signal was sent to a boxcar integrator which was operated with a personal computer.

3. Results and discussion

3.1. *Temperature dependence of SHG in FLC*

Figure 3 shows the temperature dependence of the SHG intensity in 3M2CPOOB under zero bias field. The fundamental light was directed perpendicularly on to the glass plate ($\theta = 0$). In the isotropic and smectic A phases no SHG was observed. These phases are non-ferroelectric and there is a centre of inversion symmetry.

In the cooling mode, SHG was also not observed in the chiral smectic C (S_C^*) phase in which the centre of inversion symmetry was absent. The long molecular axes of the FLC molecules tilt at an angle θ_t from the layer normal (z axis), and the tilt direction under zero bias field rotates around the layer normal from one layer to the next, resulting in a helical structure. In this structure the macroscopic cancellation of the SHG of each smectic layer results in the disappearance of the SHG.

In the heating mode, however, SHG was effective in the chiral smectic and crystalline phases. The SHG in the crystalline phase may correspond to the SHG observed by means of the powder technique in non-linear optical materials [24]. It should be noted that, even under zero field, the SHG is observed in the S_C^* phase in the

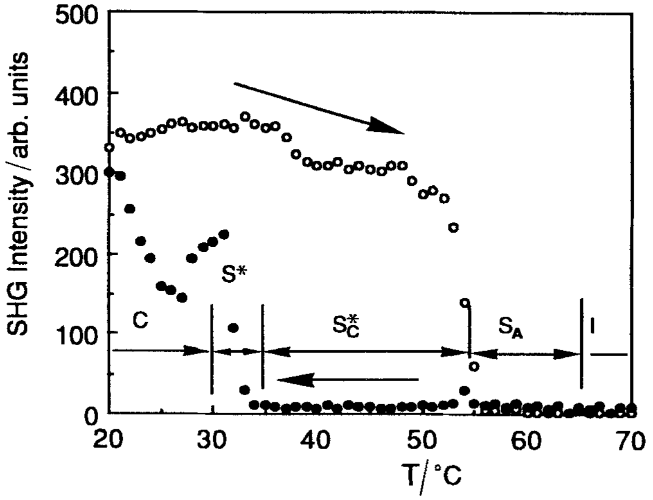

Figure 3. Temperature dependence of the SHG intensity in 34 μm thick cell of 3M2CPOOB.

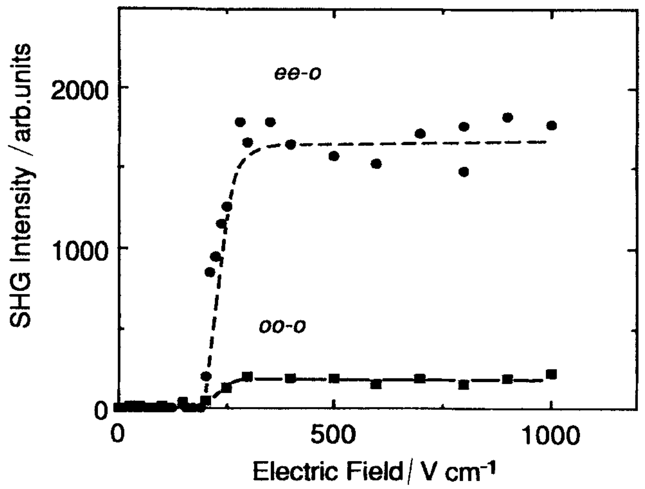

Figure 4. Electric field dependences of the SHG intensity for 3M2CPOOB in a 50 μm thick cell.

heating mode. This suggests that the structure without inversion symmetry which exists in the crystalline phase is maintained in the S_C^* phase.

3.2. *Electric field dependence of SHG in FLC*

The electric field dependence of the SHG intensity in the S_C^* phase for the rotating angle θ of about $-2{\cdot}5°$ is shown in figure 4. As is evident from this figure, the enhancement of the SHG intensity was confirmed above around 200 V cm^{-1}, which corresponds to the critical field sufficient to unwind the helical structure.

Under a DC bias field above a certain threshold, the spontaneous polarization orients along the field (y axis), and the molecules lie in the xz plane as shown in figure 2. In other words, the helical structure of the FLC is turned into the unwound structure by the electric field. In this state, the FLC has a C_2 symmetry, and dipole moments are oriented in the direction of the two fold axis normal to the molecular long axis and parallel to the smectic layer. Therefore, SHG can be observed above a critical field which is sufficient to unwind the helical structure.

Figure 4 also shows the dependence of the SHG intensity on the polarizations of the fundamental and second harmonic light. In this figure, ee-o means that two waves of the extraordinary type result in the ordinary wave of the second harmonic (the extraordinary and ordinary waves polarize in the *xz* and *yz* planes, respectively). It should be noted that only the ordinary wave of the harmonic light was observed and the extraordinary wave could not be observed. For the point group C_2, the second harmonic polarizations P_1, P_2 and P_3 along the axes 1, 2 and 3 shown in figure 2 are given by

$$\left.\begin{aligned} P_1&=2\varepsilon_0 d_{14}E_2E_3+2\varepsilon_0 d_{16}E_1E_2,\\ P_2&=\varepsilon_0 d_{21}E_1^2+\varepsilon_0 d_{22}E_2^2+\varepsilon_0 d_{23}E_3^2+2\varepsilon_0 d_{25}E_3E_1,\\ P_3&=2\varepsilon_0 d_{34}E_2E_3+2\varepsilon_0 d_{36}E_1E_2,\end{aligned}\right\} \qquad (1)$$

where d_{ij} are the elements of the second-order non-linear susceptibility tensor, ε_0 is the free space permittivity, and E_1, E_2 and E_3 are the electric field components of the fundamental wave along the dielectric axes.

For this point group, only the component of the SHG parallel to the two fold axis is permitted. Therefore, the ordinary wave (parallel to axis y) of harmonic light is the permitted component and the extraordinary wave is forbidden; this is consistent with the result shown in figure 4.

3.3. *Angular phase-matching of SHG in FLC*

Figure 5 shows the angular dependence of the SHG intensity with the electric field applied. Two extraordinary waves result in the ordinary wave of the second harmonic ee-o. Type I phase-matching of SHG was confirmed at $\theta \sim -2{\cdot}5°$. As is evident from figure 2, the phase-matching angle between the optical axis of the liquid crystal and the direction of the fundamental light, θ_m, could be estimated using the relation $\theta_m=\theta_t-\theta$, where θ_t is the tilt angle of the FLC molecules from the smectic layer normal. At this temperature, θ_t is 28° in 3M2CPOOB, and the phase-matching angle is obtained as $\theta_m = 25{\cdot}5°$. The result agrees within experimental error with the value calculated from the refractive indices, because θ_m strongly depends on the refractive indices.

It should be noted that the profile of the phase-matching curve of the SHG depends on the cell thickness and a sharp profile of the phase-matched SHG is observed for a thick cell. Although some studies on the angularly phase-matched SHG have previously been reported, in those studies, the width of the phase-matching curve was broad and the full angular width at one-half the intensity maximum of the phase-matching curve, $\Delta\theta$, was about several degrees or tens of degrees. On the other hand, neglecting beam walk-off due to the birefringence, in solid materials the phase-matching curve of the SHG depends on the sample thickness and a sharp peak is obtained for a thick sample. It is very interesting to see whether or not the sharp phase matching curve can be observed for the liquid crystal, because the liquid crystal molecules are almost freely rotating around their long axes and orientationally fluctuating.

As is evident from figure 5, in a thick cell (100 μm) a sharp phase-matched SHG was observed. Furthermore, a very sharp profile has been confirmed also in a 250 μm thick cell. This indicates that the phase-matching behaviour is hardly influenced by the free

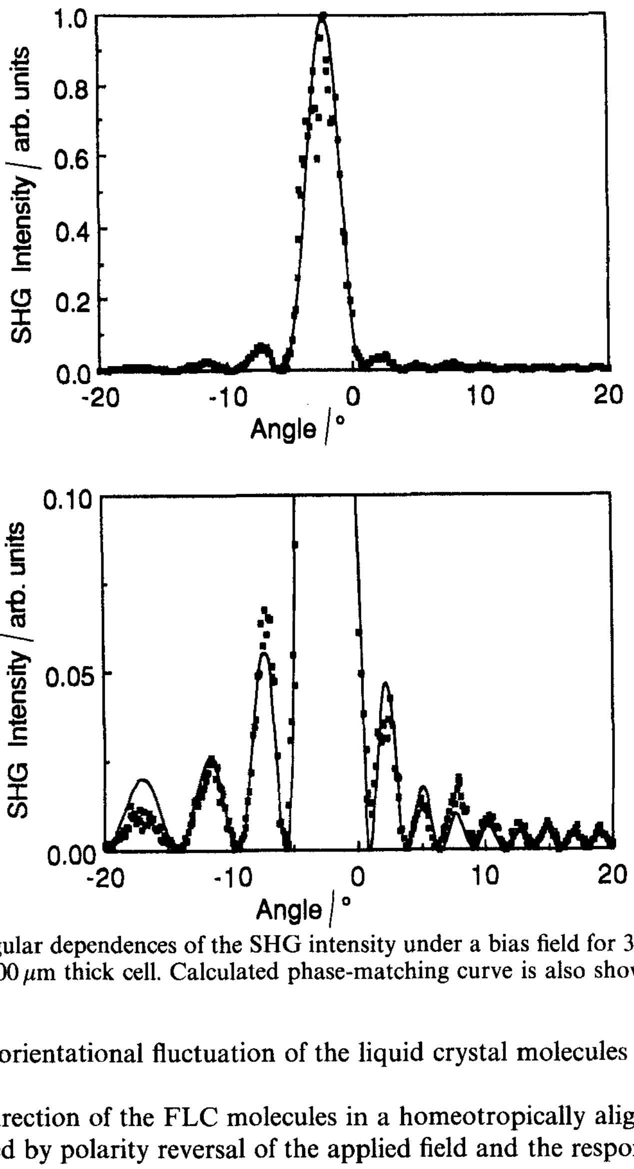

Figure 5. Angular dependences of the SHG intensity under a bias field for 3M2CPOOB in a 100 μm thick cell. Calculated phase-matching curve is also shown.

rotation and orientational fluctuation of the liquid crystal molecules even in a thick cell.

The tilt direction of the FLC molecules in a homeotropically aligned cell can be easily switched by polarity reversal of the applied field and the response time of this switching is very short [25]. This switching of the tilt direction causes the change in the matching position in the angular dependence of the SHG. In other words, phase-matched SHG is controlled by the polarity of the applied voltage. Therefore, high speed modulation of the SHG can be realized in the FLC device. Especially, faster operation may be expected by using the sharp profile of the angularly phase-matched SHG reported in this paper.

The effective non-linear coefficient d_{eff} in the present cell configuration is given by the next equation,

$$d_{\mathrm{eff}} = \varepsilon_0 d_{21} \cos^2\theta + \varepsilon_0 d_{23} \sin^2\theta + 2\varepsilon_0 d_{25} \cos\theta \sin\theta. \qquad (2)$$

At the condition of phase-matching ($\theta = \theta_{\mathrm{m}}$), $d_{\mathrm{eff}} = 0{\cdot}80 d_{21} + 0{\cdot}20 d_{23} + 0{\cdot}80 d_{25}$. In order to determine the value of d_{eff}, a relative measurement with respect to $\mathrm{LiNbO_3}$ was performed. The relative intensity and refractive indices gave $d_{\mathrm{eff}} = 0{\cdot}01\ \mathrm{pm\,V^{-1}}$. This value is small in comparison with other organic non-linear materials. However, the non-linear coefficient depends on the liquid crystal material. In particular, a liquid crystal with a large spontaneous polarization P_s does not always show large non-linear coefficients. It is necessary to design the molecular structure of the liquid crystal for the optimum SHG.

Neglecting the depletion of the fundamental light, the SHG intensity is given by

$$P_{2\omega}=\frac{2\mu_0^{3/2}}{\epsilon_0^{3/2}}\frac{P_\omega^2 d_{\mathrm{eff}}^2\omega^2 l^2}{An^3}\frac{\sin^2(\Delta kl/2)}{(\Delta kl/2)^2}, \tag{3}$$

where l is the interaction length, A is the beam area, μ_0 is free space permeability, and $\Delta k=k_{2\omega}-2k_\omega$ is the phase mismatch between the fundamental and SH waves with wave vector k_ω and $k_{2\omega}$, respectively. The theoretical fitting curve using equations (2) and (3) is also shown in figure 5, which leads to the ratio of non-linear susceptibilities for fitting parameters; $d_{23}/d_{25}=2{\cdot}3$, $d_{21}/d_{25}=0{\cdot}9$. Consequently, non-linear susceptibilities are obtained from equation (2); $d_{21}=0{\cdot}021\,\mathrm{pm\,V^{-1}}$, $d_{23}=0{\cdot}053\,\mathrm{pm\,V^{-1}}$ and $d_{25}=0{\cdot}023\,\mathrm{pm\,V^{-1}}$.

3.4. *Temperature dependence of phase-matched SHG in FLC*

The temperature dependence of the phase-matched SHG has been studied. The peak intensity of the phase-matching profile increased with decreasing temperature. Figure 6 shows the temperature dependence of d_{eff}. d_{eff} increased with decreasing temperature. Figure 6 also shows the temperature dependence of $d_{\mathrm{eff}}/\theta_t$. It is found that d_{eff} is in proportion to θ_t. This result may be explained as follows. The long axis of the FLC molecule tilts with respect to the smectic layer normal with decreasing temperature and the magnitude of the tilt angle increases monotonously. As the tilt angle increases, the free rotation around the long molecular axis is reduced, resulting in the increase in d_{eff}.

3.5. *Maker fringe in FLC*

The non-linear susceptibility d_{22} for 3M2CPOOB has been evaluated on the basis of Maker fringe measurements. Two types of cell configuration were used. That is, one

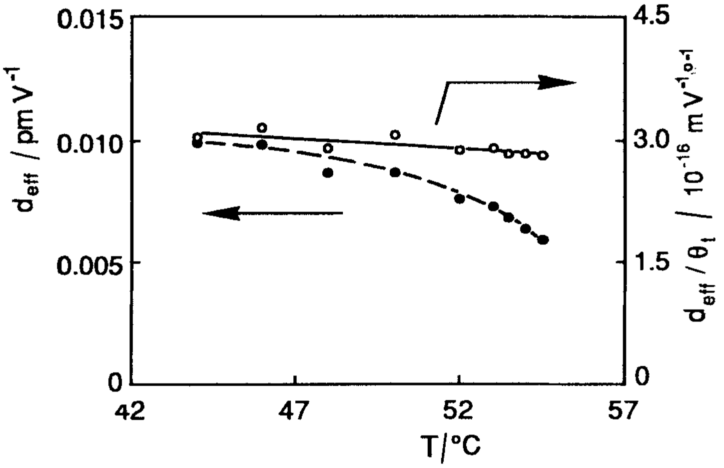

Figure 6. Temperature dependences of d_{eff} and $d_{\mathrm{eff}}/\theta_t$ for 3M2CPOOB; the cell thickness is 100 μm.

is a homeotropically aligned parallel cell which is the same as the cell used for the angular phase-matching and is rotated around the y axis. The other is a homeotropically aligned wedge cell which is shifted in the direction of the x-axis. In both cell configurations, the fundamental light and the harmonic light are ordinary waves.

Figure 7 (*a*) shows the Maker fringe profile in the parallel cell. In addition to the Maker fringe, a sharp peak was observed. The position of this peak coincides with the centre of the phase-matching curve at a corresponding temperature and is reversed with respect to the origin by the polarity reversal of the applied field. Therefore, the sharp peak in the Maker fringe, as shown in figure 7, is attributed to the phase-matched component of the SHG, due to the imperfect alignment of the molecules or smectic layers.

The coherence length l_c was determined from the positions of the fringe minima. $l_c = 12{\cdot}3\,\mu m$. The value of d_{22} can be determined from the amplitude of the fringe maxima. $d_{22} = 0{\cdot}009\,\mathrm{pm\,V^{-1}}$. d_{22} also increases with decreasing temperature.

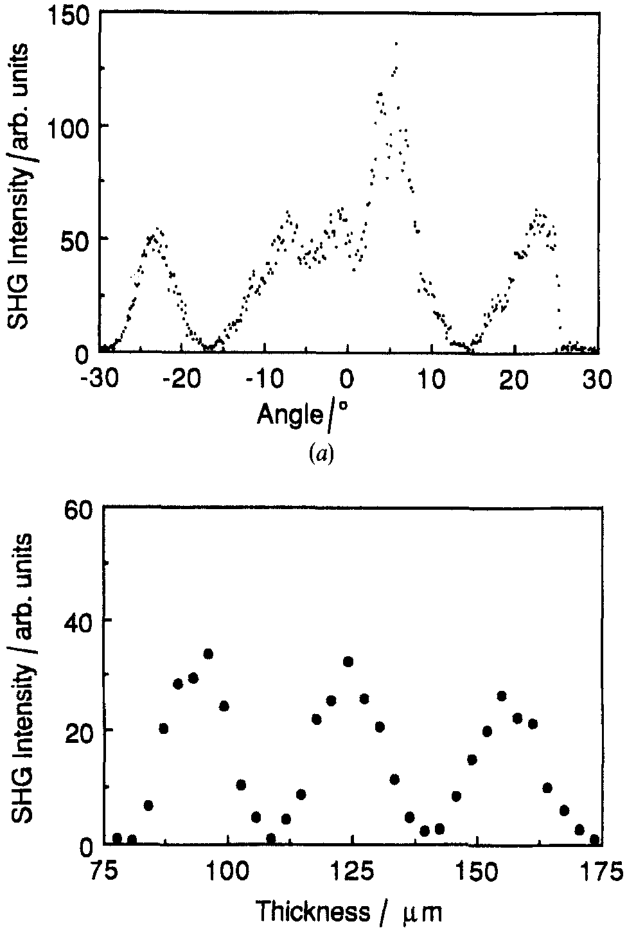

(*a*)

(*b*)

Figure 7. Maker fringe profile for d_{22} of 3M2CPOOB using (*a*) 260 μm parallel cell and (*b*) wedge cell.

3.6. *Dependence of SHG on the molecular structure*

The dependence of SHG intensity on the molecular structure of the FLC has been studied. Table 1 shows the molecular structural acronyms, spontaneous polarizations and the SHG intensities in the S_C^* phases. The SHG intensity is expressed in values relative to the phase-matched SHG intensity of 3M2CPOOB in the S_C^* phase. An obvious relationship between the molecular structure and the SHG intensity has not been observed for the compounds used in this study.

It should be noted, however, that the compounds with large P_s values such as 8, 9, 10 and 11 do not always show intense SHG. In other words, there is no obvious relation between the SHG efficiency and the magnitude of P_s. Let us take another example. In DOBA-1-MPC, a large P_s compared with that in DOBAMBC can be obtained by decreasing the distance between the chiral centre and the dipole moment, and the core and dipole moment parts are the same as those in DOBAMBC [20]. However, the SHG intensity in DOBA-1-MPC is less than that in DOBAMBC. This result indicates that the relation between the core and dipole parts may contribute to the SHG efficiency.

3.7. *Guest–host effect of SHG in FLC*

The effect of doping with dye with a large non-linearity on the SHG has been studied. Figure 8 shows the phase-matching curves of 1BC1EPOPB as a function of the concentration of *p*-nitroaniline (*p*-NA) in the FLC. A marked enhancement of SHG intensity was observed by means of slight doping with *p*-NA.

Figure 9 shows the phase-matched SHG intensity of 3M2CPOOB, 1BC1EPOPB and 1HpC1ECPOPB as a function of the concentration of *p*-NA. The SHG intensity is a relative value with respect to that of pure 3M2CPOOB. It should be noted that the SHG intensity of all FLCs are enhanced by doping with *p*-NA. In particular, the SHG intensities of 1BC1EPOPB and 1HpC1ECPOPB, which show relatively weak SHG compared with 3M2CPOOB without *p*-NA, increase on increasing the concentration of *p*-NA, and attain values over ten times as large as that without *p*-NA.

The effect of the guest dye on the SHG intensity of FLCs has been studied. Table 2 shows the relative SHG intensity of the dye-doped FLCs. *p*NA doped FLCs show the

Table 1. Spontaneous polarizations and SHG intensities for the S_C^* phases of the materials FLC used in this study. The SHG intensity is expressed in values relative to the phase-matched SHG intensity for 3M2CPOOB.

	Ps/nC cm^{-2}	SHG intensity
3M2CPOOB	−200	100·0
ETFPPOPB	150	21·0
OTFPPOPB	−90	6·0
ETFPBOB	110	—
TFHBOB	−45	—
1BC1EPOPB	240	11·0
1HpC1EPOPB	130	3·0
1MC1EPUdPB	100	6·0
1HpC1ECPOPB	−55	3·0
DOBAMBC	−5	1·2
DOBA-1-MPC	−20	0·3

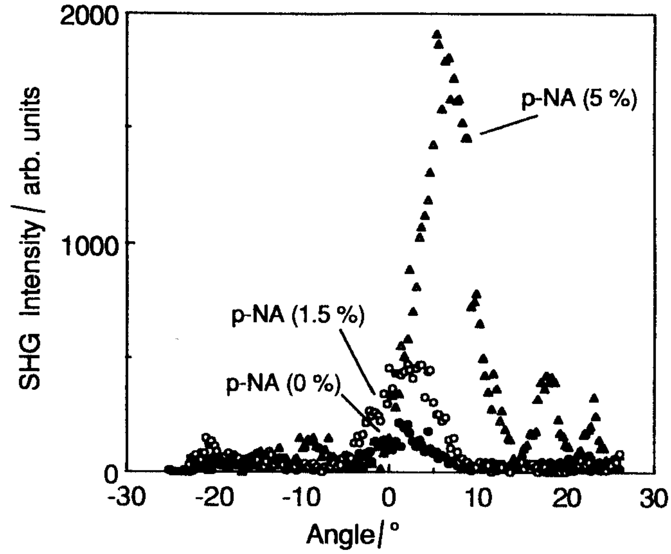

Figure 8. Phase-matching curves as a function of the concentration of *p*-NA in 1BC1EPOPB; cell thickness 34 μm and electric field 500 V cm^{-1}.

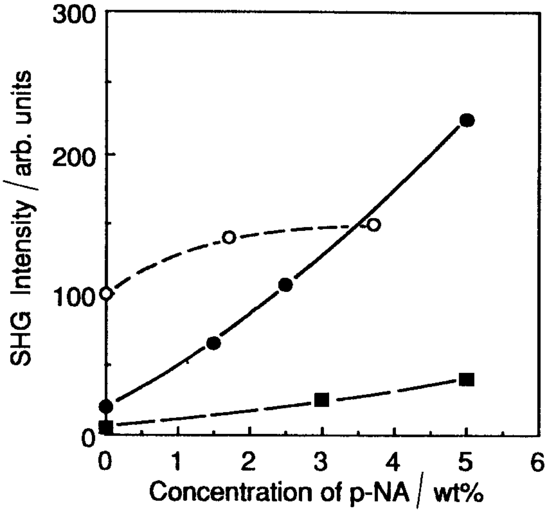

Figure 9. Dependences of SHG intensity on the concentration of *p*-NA in 3M2CPOOB (○), 1BC1EPOPB (●) and 1HpC1ECPOPB (■).

Table 2. Host effects on the SHG intensity in the doped FLCs. The SHG intensity is expressed in values relative to the phase-matched SHG intensity for pure 1BC1EPOPB.

Dye/FLC (3 wt%)	SHG intensity
1BC1EPOPB	1·0
m-NA/1BC1EPOPB	1·0
o-NA/1BC1EPOPB	2·1
4-methoxy-2-NA/1BC1EPOPB	2·3
p-NA/1BC1EPOPB	6·5

largest SHG intensity, although *o*-NA/1BC1EPOPB shows a relatively small contribution to the enhancement of SHG. However, *m*-NA does not contribute to the enhancement of SHG.

The guest effect of the enhancement of SHG may be related to the non-linearity of the guest dye. The second order hyperpolarizability β of *p*-NA ($34{\cdot}5 \times 10^{-30}$ esu) and *o*-NA ($10{\cdot}2 \times 10^{-30}$ esu) are large compared with that deduced by the vector addition of nitrobenzene and aniline, because of the intramolecular charge transfer between the donor and the acceptor group through the extended π-electron conjugated system. In *m*-NA, however, the contribution of the charge transfer is small, resulting in a small β (6×10^{-30} esu). Therefore, *p*-NA which has the largest non-linearity may contribute better to the enhancement of SHG in FLCs compared with *m*-NA with a small non-linearity. The relationship between the guest effect on the SHG and the non-linearity of this guest, as mentioned above, is also observed with related materials such as 2-methyl-4-nitroaniline and 4-methoxy-2-nitroaniline.

4. Summary

A detailed study of the SHG in FLCs was reported. It was confirmed that a sharp type I phase-matching with full angular width at one-half maximum of ~1° was realized even in a thick cell of the liquid crystal. The temperature dependences of the phase-matching behaviour and Maker fringes were also studied and non-linear optical coefficients obtained. The SHG intensity for several kinds of FLCs were measured in the S_C^* and crystalline phases. The effect of doping of dye into the FLC on the SHG was studied.

References

[1] Levine, B. F., Bethea, C. G., Thurmond, C. D., Lynch, R. T., and Bernstein, J. L., 1979, *J. appl. Phys.*, **50,** 2523.

[2] Zyss, J., Nicoud, J. F., and Coquillay, M., 1984, *J. chem. Phys.*, **81,** 4160.

[3] Wong, K. Y., and Garito, A. F., 1986, *Phys. Rev.* A, **34,** 5051.

[4] Chen, W., Feller, M. B., and Shen, Y. R., 1989, *Phys. Rev. Lett.*, **63,** 2665.

[5] Clark, N. A., and Lagerwall, S. T., 1980, *Appl. Phys. Lett.*, **36,** 899.

[6] Vtyurin, A. N., Ermakov, V. P., Ostrovskii, B. I., and Shabanov, V. F., 1981, *Phys. Stat. Sol.* B, **107,** 397.

[7] Shtykov, N. M., Barnik, M. I., Beresnev, L. A., and Blinov, L. M., 1985, *Molec. Crystal liq. Crystals*, **124,** 379.

[8] Yoshino, K., Kishio, S., Ozaki, M., Yokotani, A., Sasaki, T., and Yamanaka, C., 1987, *Tech. Rep. Osaka Univ.*, **37,** 283.

[9] Ozaki, M., Mimoto, K., and Yoshino, K., 1989, *Tech. Rep. Osaka Univ.*, **39,** 217.

[10] Taguchi, A., Ouchi, Y., Takezoe, H., and Fukuda, A., 1989, *Jap. J. appl. Phys.*, **28,** L997.

[11] Ozaki, M., and Yoshino, K., 1989, *Jap. J. appl. Phys.*, **28,** L1830.

[12] Ozaki, M., Utsumi, M., Gotou, T., Daido, K., and Yoshino, K., 1991, *Jap. J. appl. Phys.*, **30,** L1569.

[13] Liu, J. Y., Robinson, M. G., Johnson, K. M., and Doroski, D., 1990, *Optics Lett.*, **15,** 267.

[14] Liu, J. Y., Robinson, M. G., Johnson, K. M., Walba, D. M., Ros, M. B., Clark, N. A., Shao, R., and Doroski, D., 1991, *J. appl. Phys.*, **70,** 3426.

[15] Ozaki, M., Utsumi, M., Gotou, T., Morita, Y., Daido, K., Sadohara, Y., and Yoshino, K., 1991, *Ferroelectrics*, **121,** 259.

[16] Walba, D. M., Ros, M. B., Clark, N. A., Shao, R., Johnson, K. M., Robinson, M. G., Liu, J. Y., and Doroski, D., 1991, *Molec. Crystals liq. Crystals*, **198,** 51.

[17] Walba, D. M., Ros, M. B., Sierra, T., Rego, J. A., Clark, N. A., Shao, R., Wand, M. D., Vohra, R. T., Arnett, K. E., and Velsco, S. P., 1991, *Ferroelectrics*, **121,** 247.

[18] Sakurai, T., Mikami, N., Higuchi, R., Honma, M., Ozaki, M., and Yoshino, K., 1986, *Chem. Commun.*, p. 978.

[19] OZAKI, M., YOSHINO, K., SAKURAI, T., MIKAMI, N., and HIGUCHI, R., 1987, *J. chem. Phys.*, **86,** 3648.

[20] YOSHINO, K., OZAKI, M., SAKURAI, T., SAKAMOTO, K., and HONMA, M., 1984, *Jap. J. appl. Phys.*, **23,** L175.

[21] YOSHINO, K., OZAKI, M., TANIGUCHI, H., ITO, M., SATOH, K., YAMASAKI, N., and KITAZUME, T., 1987, *Jap. J. appl. Phys.*, **26,** L77.

[22] TANIGUCHI, H., OZAKI, M., YOSHINO, K., SATOH, K., and YAMASAKI, N., 1988, *Ferroelectrics*, **77,** 137.

[23] YOSHINO, K., OZAKI, M., NAKAO, K., TANIGUCHI, H., YAMASAKI, N., and SATOH, K., 1989, *Liq. Crystals*, **5,** 1203.

[24] KURTZ, S. K., and PERRY, T. T., 1968, *J. appl. Phys.*, **39,** 3798.

[25] OZAKI, M., TAGAWA, A., SADOHARA, Y., ODA, S., and YOSHINO, K., 1991, *Jap. J. appl. Phys.*, **30,** 2366.